EXPERIMENTAL CELL RESEARCH **239,** 235–242 (1998)
ARTICLE NO. EX973915

Differences in Elasticity of Vinculin-Deficient F9 Cells Measured by Magnetometry and Atomic Force Microscopy

Wolfgang H. Goldmann,*[,1] Reinhard Galneder,* Markus Ludwig,† Weiming Xu,‡ Eileen D. Adamson,‡ Ning Wang,§ and Robert M. Ezzell*

**Surgery Research Unit, Department of Surgery, Massachusetts General Hospital, Harvard Medical School, Charlestown, Massachusetts 02129; †Lehrstuhl fuer Angewandte Physik, Ludwig-Maximilians Universitaet, D-80799 Munich, Germany; ‡The Burnham Institute, La Jolla, California 92037; and §Physiology Program, Harvard School of Public Health, Boston, Massachusetts 02115*

We have investigated a mouse F9 embryonic carcinoma cell line, in which both vinculin genes were inactivated by homologous recombination, that exhibits defective adhesion and spreading [Coll *et al.* (1995) *Proc. Natl. Acad. Sci. USA* 92, 9161–9165]. Using a magnetometer and RGD-coated magnetic microbeads, we measured the local effect of loss and replacement of vinculin on mechanical force transfer across integrins. Vinculin-deficient F9Vin(−/−) cells showed a 21% difference in relative stiffness compared to wild-type cells. This was restored to near wild-type levels after transfection and constitutive expression of increasing amounts of vinculin into F9Vin(−/−) cells. In contrast, the transfection of vinculin constructs deficient in amino acids 1–288 (containing the talin- and α-actinin-binding site) or substituting tyrosine for phenylalanine (phosphorylation site, amino acid 822) in F9Vin(−/−) cells resulted in partial restoration of stiffness. Using atomic force microscopy to map the relative elasticity of entire F9 cells by 128 × 128 (n = 16,384) force scans, we observed a correlation with magnetometer measurements. These findings suggest that vinculin may promote cell adhesion and spreading by stabilizing focal adhesions and transferring mechanical stresses that drive cytoskeletal remodeling, thereby affecting the elastic properties of the cell.

Key Words: **vinculin-regulated cellular elasticity.**

INTRODUCTION

The cytoskeleton consisting of the microfilament, intermediate, and microtubule networks plays a variety of roles in the cell. It not only provides a scaffolding, where the individual elements are used as tracks for vesicular transport, but it also provides temporary binding sites for various proteins needed in vital biological processes and in concert determines the mechanical properties of the cell. The elucidation of the mechanical processes involved has shown that growth and differentiation modulate and control morphogenesis and play an important role in the generation of cell form [1, 2]. The present understanding is based on the recognition [3–6] that the mechanical integrity of the cytoskeleton largely consists of a three-dimensional interconnected protein mesh and that these fibrous units provide the mechanical links which are crucial for cell movement, form, and elasticity.

One of the links between the actin cytoskeleton and the plasma membrane, the focal adhesion plaque, consists of a complex of proteins that assemble at sites of attachment of the cell to the extracellular matrix [7]. The transmembrane proteins mediating these contacts are members of the integrin family of extracellular matrix (ECM) receptors. Integrins are heterodimeric complexes in which both chains span the plasma membrane bilayer once, and the cytoplasmic domain is responsible for linkage of the cytoskeleton. A number of proteins are found in focal adhesions at the intracellular face of the plasma membrane, including vinculin, α-actinin, paxillin, and talin. Which proteins are absolutely required for the formation of focal adhesions is still under investigation, and the order in which these proteins bind integrins, actin, or each other is only partly understood. Changes in cell shape and movement involve the transfer of mechanical forces between the cytoskeleton and the ECM as well as changes in (visco)elasticity [6, 8, 9]. The focal adhesion complex is a critical point for the regulation of actin organization as well as mechanical signal transfer. To understand the role of focal adhesion proteins with regards to cell shape change and elastic properties, it is necessary to

[1] To whom correspondence and reprint requests should be addressed at Department of Medicine, Massachusetts General Hospital/Harvard Medical School, Building 149, 13th Street, Charlestown, MA 02129. Fax: +1 (617) 726 5669. E-mail: goldman@helix.mgh.harvard.edu.

0014-4827/98 $25.00

examine the connection between the plasma membrane and the cytoskeleton. For this purpose, we have generated a F9 cell line which is deficient in vinculin using homologous recombination [10].

Vinculin is a membrane-associated protein which binds to several cytoskeletal proteins at distinct binding sites: at the NH_2-terminal end, a talin-binding site (amino acids 1–258) has been identified [11–13]. A shorter region within this fragment contains a binding site for α-actinin (amino acids 1–107) [14, 15], an actin cross-linking protein that can also bind to integrin directly [16, 17]. In the COOH-terminal region of vinculin, binding sites for paxillin (amino acids 978–1000) [18, 19], actin (amino acids 884–1012) [20–22], and acidic phospholipids (amino acids 935–978; amino acids 1020–1040) [23] have been described. The intervening central sequences in vinculin have unknown functions but include three repeats and proline-rich regions (amino acids 837–847; 860–878) [24], one of which binds to VASP [25, 26]. The molecule is thought to form a globular head domain and an extended tail domain that can fold to mask the principal binding domains [21].

To investigate the mechanical linkage of the focal adhesion complex with the cytoskeleton, we here used a magnetic twisting device to apply controlled mechanical stresses directly via integrin cell surface receptors producing local changes in cell shape. Shear stress (torque) was applied to membrane-bound ferromagnetic microbeads (4.5 μm in diameter) that were coated with ligands for the cell surface receptor. The cellular deformation that resulted in response to stress application was determined by simultaneously quantifying bead rotation (angular strain) using an in-line magnetometer [27].

To examine the elastic properties of these cell lines we used the atomic force microscope (AFM). This device has proven to be an effective tool for investigating the motility of living cells [28–30]. A major advantage of this noninvasive method is its ability to detect morphologic and dynamic changes in the elastic properties of the whole cell with a high resolution. The AFM scans the cell surface using a sharp tip at the end of a cantilever. At low scanning forces (force mapping mode) the cell's topography is determined, and higher forces allow for measurements of the local elasticity. The AFM has been used to examine the surface morphology and mechanical properties of MDCK cell monolayers [31] and human platelets [32, 33].

The goal of this work is to determine the (visco)elastic properties of vinculin in cells. Magnetometry experiments will measure local changes in cell stiffness by examining a specific receptor–ligand interaction (i.e., of RGD-coated magnetic beads binding to integrins), while atomic force microscopy will be used to obtain information on the role of vinculin in the elasticity of the entire cell. For this purpose we used F9 cells deficient in vinculin, F9Vin(−/−). Stable transfectants of these cells with a plasmid that expresses full-length vinculin, or vinculin with an NH_2-terminal deletion, or mutant vinculin were also compared for changes in stiffness and elasticity. Studying vinculin in F9 cells will provide a unique opportunity to define the physical properties.

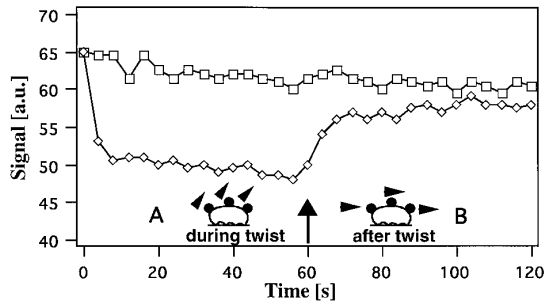

FIG. 1. Typical response of cultured F9Vin(−/−) cells obtained using magnetic twisting cytometry. In the absence of the applied twisting field (top trace, squares) the magnetic signal (a.u., arbitrary units) exhibits only a small decrease in signal, which is probably due to thermal motion and membrane movement. However, in a constant twisting field (bottom trace, diamonds) at 30 G, which was applied in the vertical direction for 60 s (A), the magnetic signal of the beads decreased almost instantaneously. By subtracting the relaxation signal from the control [48], the remanent field signal almost reached a plateau after 60 s. This signal is then used to calculate the apparent stiffness. After the twisting field is turned off (B), the remanent field quickly increases returning toward the value at $t = 0$. This indicates that marked elastic energy is stored in the cell, allowing it to recover almost to the original energy level. The difference in signal in (top) and (bottom) after 120 s (incomplete recovery) is probably due to the "impure elastic material" and exhibits some permanent deformation. The inset gives a schematic view of the principle of the magnetic twisting device. Note: the orientation of the beads is indicated by the arrows.

MATERIALS AND METHODS

Cell lines. Full-length mouse vinculin cDNA was made by polymerase chain reaction (PCR), and F9Vin(−/−) cells—also called γ229—were transfected with the cDNA by the Ca^{2+}–phosphate precipitation method. Using vector β-actin promoter/CMV enhancer (CXN2 vector, [34]) driving the mouse vinculin cDNA, different levels of vinculin expression were achieved: R16 = 21% and R3 = 83%. We also constructed this vector in versions that express (i) vinculin minus the talin- and α-actinin-binding site (amino acids 289–1066), called Tal8; and (ii) the full-length version of mouse vinculin with a mutation that converts a known phosphorylation site (amino acids 822, tyrosine) into phenylalanine, called M4. The level of vinculin expressed by these clones was determined quantitatively by immunoblotting and Western blotting.

Cell culture. The wild-type, F9Vin(−/−), and all transfected cells and cell constructs were maintained on 0.1% gelatin-coated charged plastic culture dishes in high-glucose (4.5 g/L) Dulbecco's modified Eagle's medium supplemented with 10% calf serum, 20 mM Hepes,

2 mM L-glutamine, and 100 U/ml penicillin–streptomycin (P/S). Chemicals were supplied by Sigma (St. Louis, MO); petri dishes were provided by CorningGlass Works (Corning, NY) and trypsin and P/S were supplied by Gibco (Gaitherburg, MD).

Magnetometry. This device has previously been described [27]. In brief, F9 cells were plated (15×10^4 cells per well) on 2 μg/ml poly-D-lysine-coated plastic wells (96 Removawells, Immunolon, IL) and cultured for 12 h before addition of 4.5-μm spherical ferromagnetic beads that were precoated with a synthetic RGD-containing peptide (Peptide 2000, Telios Pharmaceuticals, La Jolla, CA), which is a specific ligand for integrin receptors. After 10 min, unbound beads were washed away with 1% BSA, and the wells were then placed into the magnetic twisting device and maintained at 37°C. To completely magnetize the ferromagnetic beads, a brief (10 μs) but strong (1000 G) homogeneous magnetic pulse was applied. After 20 s a magnetic twisting field was applied in the vertical direction for 1 min, the beads were twisted, and the direction was measured by a torque (Fig. 1, inset) [35]. An in-line magnetometer was used to detect the magnitude of the bead magnetic vector. The twisting field was then turned off for 1 min, and the extent of recovery of the bead magnetic signal was measured (Figs. 1A and 1B). The stiffness was determined according to a method described in [35].

Atomic force microscopy. The atomic force microscope is a home-built instrument (Fig. 2). In brief, this instrument is combined with an epi-light microscope that allows the exact positioning of the cantilever tip. The deflection of the cantilever is measured by a position-sensitive two-segment photo diode, and the extent to which the applied force indents the cells depends on their elastic properties. The Hertz model was used to describe the elastic response of F9 cell lines indented by the AFM cantilever which predicts a relation between indentation and loading force [33]. The image area was determined by 128×128 ($n = 16{,}384$) pixels. At each pixel point, the deflection signal of the cantilever was analyzed for the topography and elasticity of the cell. The variation in 0–255 "elastic" scales and the color images were generated by transferring the data into pseudo-colors, where blue corresponds to hard and red to soft. Three dimensional profiles were generated by using a customized processing software "Image 1.41b20 (non FFT)" and Adobe Photoshop 3.0.

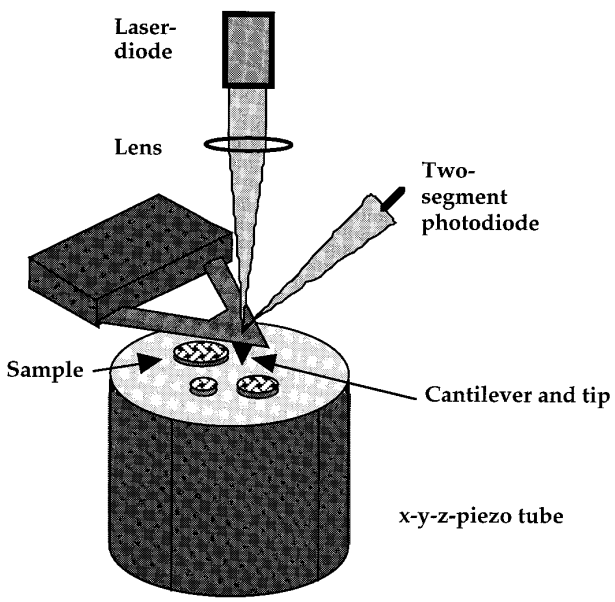

FIG. 2. Schematic diagram of an atomic force microscope consisting of a laser diode, lens, cantilever and tip, two-segment photo diode, *x-y-z*-piezo tube, and sample.

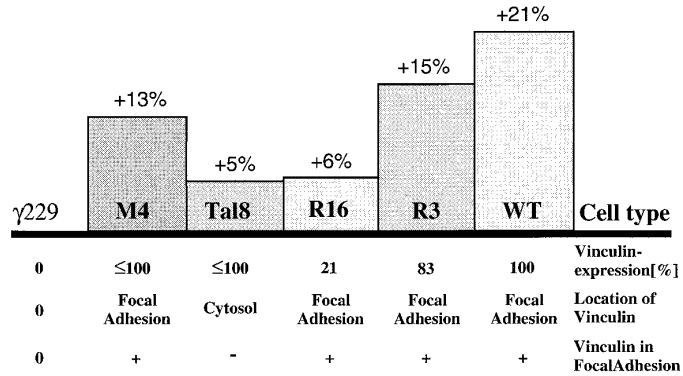

FIG. 3. The stiffness, shown as a percentage, determined by magnetometry for M4 [phosphorylation site, amino acid 822 (tyrosine) substituted with phenylalanine], Tal8 [transfected F9Vin(−/−) cell with the vinculin construct, missing amino acids 1–288], vinculin-deficient F9Vin(−/−) cells, R16 and R3, expressing 21 and 83% vinculin, as well as wild-type cells is set relative to vinculin-deficient F9 Vin(−/−), called γ229 cells. An average of $n = 25$ separate measurements per cell line were carried out, showing a standard deviation of SD $< 3\%$. Vinculin expression was measured by immunoblotting relative to F9 wild-type cells. The location of vinculin in cells was observed by confocal microscopy, and the adhesion was measured by cell attachment to fibronectin (5 μg/ml) in 96-well plates as described previously [10].

RESULTS

Magnetometry. Prior to measurements using the different F9 cell lines, we calibrated the magnetic twisting device to enable us to calculate the apparent stiffness (Fig. 1 and inset). Here, the RGB-coated magnetic beads attached to integrins of wild-type F9 cells are briefly magnetized in the horizontal direction before a magnetic field in the vertical direction for 60 s is applied. The extent of the bead rotation is then determined by quantifying the change in remanent field (=difference in signal amplitudes).

Figure 3 shows the relative stiffness of vinculin-deficient F9Vin(−/−) cells, called γ229, to γ229 expressing mutant vinculin Y822F, (M4); γ229 expressing vinculin with deleted sequences 1–288 (Tal8); and full-length vinculin rescued clones (R3 and R16), and wild-type F9 cells. It depicts the changes in relative stiffness which differ by 21% for wild-type and vinculin-deficient F9 Vin(−/−) cells. Transfecting F9 Vin(−/−) cells with full-length cDNA, in which a tyrosine phosphorylation site of vinculin is substituted by one amino acid (M4), shows a notable effect in relative stiffness. However, when F9 Vin(−/−) cells expressed a truncated vinculin, which is deficient in the talin- and α-actinin-binding site (clone Tal 8), the relative stiffness increased only

by 5% compared to vinculin-deficient F9 Vin(−/−) cells. F9 Vin(−/−) cells expressing 21% (R16) and 83% (R3) of vinculin compared to wild-type cells indicate a clear trend that with rising vinculin concentration the relative stiffness increases. At 83% vinculin expression, the relative stiffness reached almost wild-type levels.

Atomic force microscopy. Prior to examination, the F9 cell lines are cultured for 8 h on 2 μg/ml poly-D-lysine coated 35 × 15 mm NUNC dishes and placed on a (*x*-*y*-*z*-piezo) stage during atomic force microscopy (Fig. 2). In a typical experiment, the light emitted from the laser is focused on the cantilever tip as it raster-scans across the cell, and a position-sensitive photodiode measures the deflection of the cantilever. The extent to which the applied force indents the cell surface depends on the elastic properties, and a motif of the cell is created which is made up of 128 × 128 data points. These points are then translated into 256 scales to produce a topographic image and to quantify the elasticity of the cell.

Figure 4 represents the three-dimensional profiles in pseudo-colors which were generated by 16,384 force scans. As indicated by the color scale (on right), the wild-type cell (Fig. 4A) is less deformed by the cantilever (and thus harder) in comparison to the F9Vin(−/−) cell (Fig. 4B). The total area of the F9Vin(−/−) cell shows less than 80% of the wild-type level and much reduced lamellipodia and with numerous filopodia which were also observed by light microscopy [10, 36]. In Fig. 4C, the R16 cell indicates a shift to "harder" distribution which almost reaches the wild-type level in R3 cells (Fig. 4D). The M4 cell (Fig. 4E) shows a moderate increase in elasticity with lamellipodia as well as filopodia distributions similar to those of the wild-type cell. Figure 4F shows the Tal8 cell line, which is deficient in amino acids 1–288 (NH_2-terminal region) and which only partially restores the elasticity of the cell. (Note: the elastic distribution is calculated from 256 original elastic scales, where 0 is defined as soft and 255 as hard for all cell lines and a total of 16,384 pixels per image).

Figure 5 shows the relative elasticity of the various cell lines in comparison to vinculin-deficient F9 Vin(−/−) cells. Here, a similar trend is observed for the elastic behavior of a whole cell compared to local cell stiffness measured by magnetometry insofar as the reduction of vinculin in the cell and the expression of vinculin fragments have an influence on cell stiffness/elasticity. Most noticeable, however, is that the mutation of a single tyrosine residue or the absence of the talin- and α-actinin-binding sites on vinculin markedly affects the relative elasticity and the relative stiffness (Fig. 3) and shows the importance of these functional domains of vinculin to the cell characteristics. These findings support the assumption made by Ezzell *et al.* [37] that vinculin has an influence on the elastic behavior of F9 cells.

DISCUSSION

The importance of vinculin in the focal adhesion complex and in specialized cell types has previously been described for different cells. Rodriguez Fernandez *et al.* [38] reduced vinculin expression in mouse 3T3 cells, and the transfected cells exhibited a round phenotype with fewer vinculin-positive focal contacts and displayed increased motility. Varnum-Finney and Reichardt [39] showed that vinculin-deficient PC12 cells produce unstable filopodia and lamellipodia and have a reduced rate of neurite outgrowth. A similar situation is observed also in F9Vin(−/−) cells. Here, the loss of vinculin resulted in rounded morphology, decreased adhesion, and increased motility [10]. All these studies suggested that vinculin is probably critical for normal cell attachment and spreading and that other mechanisms in the formation of focal adhesion plaques may also exist. Possible candidates are talin and α-actinin, which bind to actin, vinculin, and each other [40].

In this work we have examined the influence of different vinculin expression and vinculin constructs on the mechanical properties of F9 cells measuring local stiffness and the elasticity of entire cells. The data from the magnetometer and atomic force microscope analyses agree generally insofar as the lack of vinculin in F9Vin(−/−) cells reflects changes in phenotype (Fig. 4) which correlate with a decrease in cell stiffness/elasticity. A more specific explanation of the influence of vinculin on the elastic properties can be made by observations of the rescue cells (R3 and R16). Here, with decreasing vinculin concentration the relative stiffness/elasticity decreases to almost the F9Vin(−/−) level (Figs. 3 and 5). It is likely that larger amounts of vinculin within the cell lead to more stable molecular structures of the focal adhesion complex, which then result in better cell spreading. We have observed that the full reconstitution of wild-type properties (i.e., spreading, locomotion, adhesion) is affected by the expression of whole intact vinculin. Interestingly, normal adhesion was restored by as little as 9% of typical vinculin levels and was no different from that in cells that expressed 83% levels (Fig. 3 and Ref. [41]).

The observations of Volberg *et al.* [36] indicate that the vinculin-negative F9 cells compensate for this lack by up-regulating the levels of α-actinin, talin, and paxillin in the focal adhesion complexes (FACs) by 30%. We believe that this increase in FACs affects some of the characteristics of the rescued cells. For example, when vinculin expression is restored with the full-length molecule, the number and size of the FACs are noticeably greater than those of wild-type cells, sug-

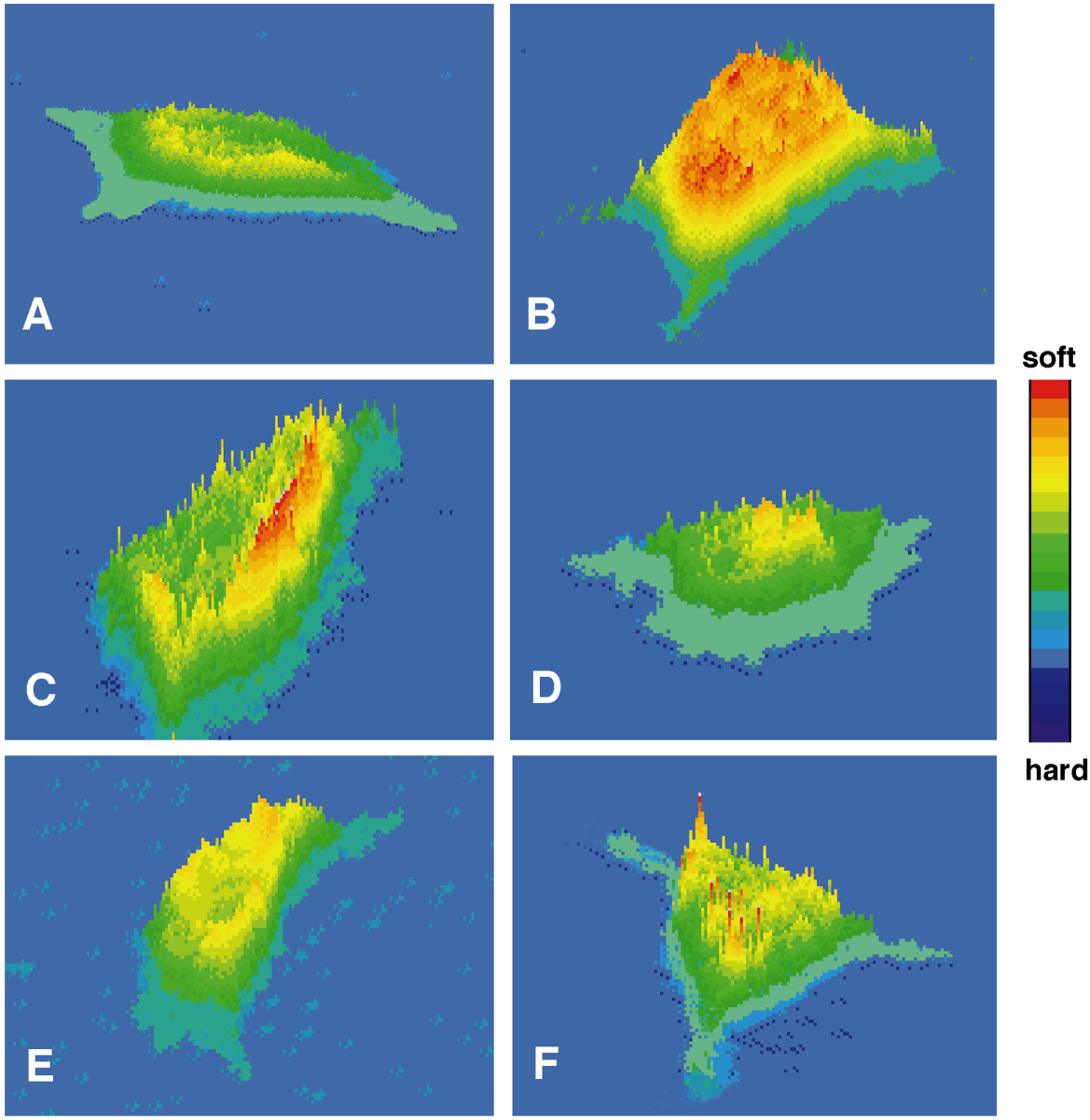

FIG. 4. Results from atomic force microscopy of wild-type F9 (A), F9Vin(−/−), also called γ229 (B), vinculin-transfected cells, R16 (C), vinculin-transfected cells, R3 (D), M4 (E), and Tal8 (F). The three-dimensional profiles were generated by 128 × 128 (=16,384) force scans of the cantilever. As indicated by the pseudo-color scale (right), the wild-type cell (A) is less deformed by the cantilever (and thus harder) in comparison to the F9Vin(−/−) cell (B). (C and D) Transfection with intact vinculin expressing 21 and 83% vinculin restored the spatial elasticity, whereas tyrosine substituted with phenylalanine (amino acid 822, phosphorylation site) and transfection with missing amino acids 1–288 (Tal8) only partially restore the elasticity of the cell (E and F, respectively).

gesting that vinculin binds to the "extra" talin, α-actinin, and paxillin in the FACs. This may explain why 9% of normal levels of vinculin restored adhesion to wild-type levels (Fig. 3 and Ref. [41]). Introduction of NH_2-truncated vinculin to the vinculin null cells (Tal8) did not rescue the stiffness, elasticity, or adhesion to fibronectin. Confocal microscopy showed that the truncated vinculin in these cells was not in the FACs and that the cells remained rounded and unspread. The difference in cell stiffness and elasticity observed for Tal8 (Figs. 3 and 5) may be attributed to the measuring techniques, as magnetometry detects more local changes of the cell and atomic force microscopy detects more global changes of the cell. From this, we can conclude that the talin- and α-actinin binding sites are important for all the properties of vinculin. These find-

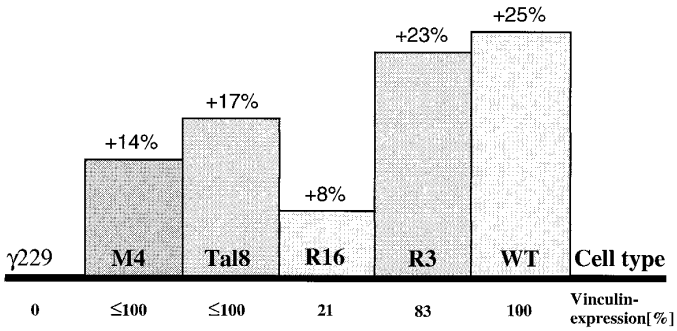

FIG. 5. Relative changes in elasticity (%) of vinculin-substituted M4, vinculin-construct Tal8, vinculin-transfected R16 and R3, and wild-type F9 cells to vinculin-deficient F9Vin(−/−), also called γ229, cells measured by the atomic force microscope. Number of analyzed cells, $n = 5$; standard deviation, SD < 3%. The relative elastic changes (in %) of the entire cells are consistent with relative changes in local cell stiffness (Fig. 3).

ings also imply that the binding of vinculin to talin and α-actinin is a necessary connection in stabilizing the FAC.

The M4 cells expressed a mutant vinculin, in which the phosphorylation site (Tyr 822) was changed to Phe. Compared to γ229, the vinculin null cell from which they were derived, there was a moderate improvement in relative stiffness/elasticity. In this case, the vinculin was located in the FAC (data not shown), but it was inactive in restoring adhesion and locomotion to normal F9 wild-type levels. On the contrary, these remained unchanged from the properties of F9Vin(−/−) cells. It is possible therefore, that the location of vinculin (even mutant vinculin) in FACs has a positive effect on cell stiffness and elasticity. Only the results of clone R16 argue against this and suggest that this cell line may have other defects that we have not yet detected.

We recently compared the protein content and the focal adhesion proteins, i.e., talin, α-actinin, paxillin, and actin, in another mutant F9 cell line (5.51) that lacks vinculin with wild-type cells and two different vinculin-transfected clones [42, 43]. Interestingly, the 5.51 cells that lacked vinculin retained the ability to form filopodia and contained normal levels of total polymerized and cross-linked actin, yet they could not form lamellipodia, assemble stress fibers, or efficiently spread when plated on the extracellular matrix. Furthermore, when vinculin was replaced by transfection, the stress fiber formation and cell spreading were restored to near wild-type levels. A similar trend was observed when measuring the physical properties of these cell lines. The stiffness and elasticity in 5.51 cells decreased by ≥50% and ~20%, respectively, and returned to near wild-type levels in vinculin-transfected 5.51 cells ([37, 44] and data not shown). These findings are in general agreement with observations made in this study, although the change in stiffness was less pronounced in F9Vin(−/−) cells.

Previously, Wang *et al.* [35, 45] have shown that cell adhesion molecules can mediate force transfer across the cell surface and to the cytoskeleton. In addition, these authors have been able to demonstrate that mechanical coupling between integrin and the cytoskeleton is observed in many cell types and that the stiffening response is accompanied by coordinated changes in cytoskeleton mechanics. Other laboratories have also confirmed that focal adhesion proteins physically couple to the cytoskeleton [46] and that they transfer cytoskeletal tension to the extracellular matrix [47]. All in all, these results and data from experiments in this study may support the hypothesis that the (visco)elastic properties of the cell correlate with recruitment of focal adhesion proteins and, thus, physical linkage of integrins to the actin cytoskeleton.

We thank Dr. Manfred Radmacher for helpful comments and Judith Feldmann for proof-reading the manuscript. This work was supported by the American Cancer Society, NASA NAG5-4839, NIH HL-33009, Deutsche Forschungsgemeinschaft Go 598/3-1, and NATO (CRG 970205). Excerpts of this work were presented at the annual ASCB Meeting (1996) in San Francisco as a poster and published in abstract form in *Mol. Biol. Cell* (1996) **7S,** 385a.

REFERENCES

1. Ingber, D. E., and Folkman, J. (1989). How does extracellular matrix control capillary morphogenesis? *Cell* **58,** 803–805.
2. Ettinger, L., and Doljanski, F. (1992). On the generation of form by the continuous interaction between cells and their extracellular matrix. *Biol. Rev.* **67,** 459–489.
3. Rasmussen, S., Karampurwala, H., Vaidyanath, R., Jensen, K. S., and Hameroff, S. (1990). Computational connectionism within neuroses: A model of cytoskeletal automata subserving neural networks. *Physica* **D42,** 428–449.
4. Bereiter-Hahn, J. (1991). Cytomechanics and biochemistry. Springer-Verlag, Berlin.
5. Ingber, D. E., Karp, S., Plopper, G., Hansen, L., and Mooney, D. (1993). Mechanochemical transduction across extracellular matrix and through the cytoskeleton. *In* "Physical Forces and the Mammalian Cell," pp. 61–79, Academic Press, San Diego.
6. Isenberg, G. (1996). New concepts for signal perception and transduction by the actin cytoskeleton at cell boundaries. *Semin. Cell Dev. Biol.* **7,** 707–715.
7. Jockusch, B. M., Bubeck, P., Giehl, K., Kroemker, M., Moschner, J., Rotkegel, M., Ruediger, M., Schiller, K., Stanke, G., and Winkler, J. (1995). The molecular architecture of focal adhesions. *Annu. Rev. Cell Dev. Biol.* **11,** 379–416.
8. Ingber, D. E., Dike, L., Hansen, L., Karp, S., Liley, H., Maniotis, A., McNamee, H., Mooney, D., Plopper, G., Sims, J., and Wang, N. (1994). Cellular tensegrity: Exploring how mechanical changes in the cytoskeleton regulate cell growth, migration, and tissue pattern during morphogenesis. *Int. Rev. Cytol.* **150,** 173–224.
9. Mooney, D. J., Langer, R., and Ingber, D. E. (1995). Cytoskeletal

filament assembly and the control of cell spreading and function by extracellular matrix. *J. Cell Sci.* **108,** 2311–2320.

10. Coll, J. L., Ben-Ze'ev, A., Ezzell, R. M., Rodriguez Fernandez, J. L., Baribault, H., Oshima, R. G., and Adamson, E. D. (1995). Targeted disruption of vinculin genes in F9 and embryonic stem cells changes cell morphology, adhesion, and locomotion. *Proc. Natl. Acad. Sci. USA* **92,** 9161–9165.
11. Burridge, K., and Mangeat, P. H. (1984). An interaction between vinculin and talin. *Nature* **308,** 744–746.
12. Critchley, D. R., Gilmore, A., Hemmings, L., Jackson, P., McGregor, A., Ohanian, V., Patel, B., Waites, G., and Wood, C. (1991). Cytoskeletal proteins in adherens-type cell–matrix junctions. *Biochem. Soc. Trans.* **19,** 1028–1033.
13. Gilmore, A. P., Jackson, P., Waites, G. T., and Critchley, D. R. (1992). Further characterization of the talin-binding site in the cytoskeletal protein vinculin. *J. Cell Sci.* **103,** 719–731.
14. Belkin, A. M., and Koteliansky, V. E. (1987). Interaction of iodinated vinculin, metavinculin, and alpha-actinin with cytoskeletal proteins. *FEBS Lett.* **220,** 291–294.
15. Menkel, A. R., Kroemker, M., Bubeck, P., Ronsiek, M., Nikolai, G., and Jockusch, B. M. (1994). Characterization of an F-actin-binding domain in the cytoskeletal protein vinculin. *J. Cell Biol.* **126,** 1231–1240.
16. Otey, C. A., Pavalko, F. M., and Burridge, K. (1990). An interaction between alpha-actinin and the beta-1 integrin subunit in vitro. *J. Cell Biol.* **111,** 721–729.
17. Pavalko, F. M., and Burridge, K. (1991). Disruption of the actin cytoskeleton after microinjection of proteolytic fragments of α-actinin. *J. Cell Biol.* **114,** 481–491.
18. Turner, C. E., Glenney, J. R., Jr., and Burridge, K. (1990). Paxillin: A new vinculin-binding protein present in focal adhesions. *J. Cell Biol.* **111,** 1059–1068.
19. Wood, C. K., Turner, C. E., Jackson, P., and Critchley, D. R. (1994). Characterisation of the paxillin-binding site and the C-terminal focal adhesion targeting sequence in vinculin. *J. Cell Sci.* **107,** 709–717.
20. Johnson, R. P., and Craig, S. W. (1994). An intramolecular association between the head and tail domains of vinculin modulates talin binding. *J. Biol. Chem.* **269,** 12611–12619.
21. Johnson, R. P., and Craig, S. W. (1995). F-actin binding site masked by the intramolecular association of vinculin head and tail domains. *Nature* **373,** 261–264.
22. Kroemker, M., Ruediger, A. H., Jockusch, B. M., and Ruediger, M. (1994). Intramolecular interactions in vinculin control alpha-actinin binding to the vinculin head. *FEBS Lett.* **355,** 259–262.
23. Tempel, M., Goldmann, W. H., Isenberg, G., and Sackmann, E. (1995). Interaction of the 47-kDa talin fragment and the 32-kDa vinculin fragment with acidic phospholipids: A computer analysis. *Biophys. J.* **69,** 228–241.
24. Moiseyeva, E. P., Weller, P. A., Zhidhova, N. I., Corben, E. B., Patel, B., Jasinska, I., Koteliansky, V. E., and Crichtley, D. R. (1993). Organization of the human gene encoding the cytoskeletal protein vinculin and the sequence of the vinculin promoter. *J. Biol. Chem.* **268,** 4318–4325.
25. Reinhard, M., Ruediger, M., Jockusch, B. M., and Walter, U. (1996). VASP interaction with vinculin: A recurring theme of interactions with proline-rich motifs. *FEBS Lett.* **399,** 103–107.
26. Brindle, N. P. J., Holt, M. R., Davies, J. E., Price, C. J., and Critchley, D. R. (1996). The focal-adhesion vasodilator-stimulated phosphoprotein (VASP) binds to the proline-rich domain in vinculin. *Biochem. J.* **318,** 753–757.
27. Wang, N., Butler, J. P., and Ingber, D. E. (1993). Mechanotransduction across the cell surface and through the cytoskeleton. *Science* **260,** 1124–1127.
28. Keller, D. L., Chang, K. L., Singh, S., and Yorganciogla, M. (1992). Scanning force microscopy of cells and membrane proteins. *Proc. SPIE* **1639,** 91–101.
29. Radmacher, M., Tillmann, R. W., Fritz, M., and Gaub, H. E. (1992). From molecules to cells—Imaging soft samples with the AFM. *Science* **257,** 1900–1905.
30. Hansma, H. G., and Hoh, J. H. (1994). Biomolecular imaging with the atomic force microscope. *Annu. Rev. Biophys. Chem.* **23,** 115–139.
31. Schoenenberger, C.-A., Zuk, A., Zinkl, G. M., Kendall, D., and Matlin, K. S. (1994). Integrin expression and localization in normal MDCK cells and transformed MDCK cells lacking apical polarity. *J. Cell Sci.* **107,** 527–541.
32. Fritz, M., Radmacher, M., and Gaub, H. E. (1993). In vitro activation of human platelets triggered and probed by SFM. *Exp. Cell Res.* **205,** 187–190.
33. Radmacher, M., Fritz, M., Kacher, C. M., Cleveland, J. P., and Hansma, P. K. (1996). Measuring the viscoelastic properties of human platelets with the atomic force microscope. *Biophys. J.* **70,** 556–567.
34. Niwa, H., Yamamura, K., and Miyazaki, J. (1991). Efficient selection for high-expression transfectants with a novel eukaryotic vector. *Gene* **108,** 193–199.
35. Wang, N., and Ingber, D. E. (1994). Control of cytoskeletal mechanics by extracellular matrix, cell shape, and mechanical tension. *Biophys. J.* **66,** 2181–2189.
36. Volberg, T., Geiger, B., Kam, Z., Pankov, R., Simcha, I., Sabanay, H., Coll, L. J., Adamson, E. D., and Ben-Ze'ev, A. (1995). Focal adhesion formation by F9 embryonal carcinoma cells after vinculin gene disruption. *J. Cell Sci.* **108,** 2253–2260.
37. Ezzell, R. M., Goldmann, W. H., Wang, N., Parasharama, N., and Ingber, D. E. (1997). Vinculin promotes cell spreading by mechanically coupling integrins to the cytoskeleton. *Exp. Cell Res.* **231,** 14–26.
38. Rodriquez Fernandez, J. L., Geiger, B., Salomon, D., and Ben-Ze'ev, A. (1993). Suppression of vinculin expression by antisense transfection confers changes in cell morphology, motility, and anchorage-dependent growth of 3T3 cells. *J. Cell Biol.* **122,** 1285–1294.
39. Varnum-Finney, B., and Reichardt, L. F. (1994). Vinculin-deficient PC12 cell lines extend unstable lamellipodia and filopodia and have a reduced rate of neurite outgrowth. *J. Cell Biol.* **127,** 1071–1084.
40. Goldmann, W. H., Ezzell, R. M., Adamson, E. D., Niggli, V., and Isenberg, G. (1996). Vinculin, talin and focal adhesions. *J. Muscle Res. Cell Motil.* **17,** 1–5.
41. Xu, W., Coll, J. L., and Adamson, E. D. (1997). Vinculin function as a molecular bridge in cell signaling: Expression of vinculin head or tail domains in vinculin null F9 cells have opposite effects on cell locomotion. Submitted for publication. [in revision]
42. Samuels, M., Ezzell, R. M., Cardozo, T. J., Critchley, D. R., Coll, J. L., and Adamson, E. D. (1993). Expression of chicken vinculin complements the adhesion-defective phenotype of a mutant mouse F9 embryonal carcinoma cell. *J. Cell Biol.* **121,** 909–921.
43. Goldmann, W. H., Schindl, M., Cardozo, T. J., and Ezzell, R. M. (1995). Motility of vinculin-deficient F9 embryonic carcinoma cells analyzed by video, laser confocal, and reflection interference contrast microscopy. *Exp. Cell Res.* **221,** 311–319.
44. Goldmann, W. H., and Ezzell, R. M. (1996). Viscoelasticity in

wild-type and vinculin-deficient (5.51) mouse F9 embryonic carcinoma cells examined by atomic force microscopy and rheology. *Exp. Cell Res.* **226,** 234–237.

45. Wang, N., and Ingber, D. E. (1995). Probing transmembrane mechanical coupling and cytomechanics using magnetic twisting cytometry. *Biochem. Cell. Biol.* **73,** 1–9.
46. Schmidt, C. E., Horwitz, A. F., Lauffenburger, D. A., and Sheetz, M. P. (1983). Integrin-regulated cytoskeletal interactions in migrating fibroblasts are dynamic, asymmetric and regulated. *J. Cell Biol.* **123,** 977–991.
47. Schiro, J. A., Chan, B. M., Roswit, W. T., Kassner, P. D., Pentland, A. P., Hemler, M. E., Eisen, A., and Kupper, T. S. (1991). Integrin $\alpha 2\beta 1$ (VLA-2) mediaters reorganization and contraction of collagen matrices by human cells. *Cell* **67,** 403–410.
48. Valberg, P. A., and Butler, J. P. (1987). Magnetic particle motions within living cells: Physical theory and techniques. *Biophys. J.* **52,** 537–550.

Received October 16, 1997
Revised version received November 26, 1997